Precision X-ray Timing of RX J0806.3+1527 with CHANDRA: Evidence for Gravitational Radiation from an Ultracompact Binary

Tod E. Strohmayer

Laboratory for High Energy Astrophysics, NASA's Goddard Space Flight Center, Greenbelt, MD 20771; stroh@clarence.gsfc.nasa.gov

ABSTRACT

RX J0806.3+1527 is a candidate double degenerate binary with possibly the shortest known orbital period. The source shows an $\approx$ 100% X-ray intensity modulation at the putative orbital frequency of 3.11 mHz (321.5 s). If the system is a detached, ultracompact binary gravitational radiation should drive spin-up with a magnitude of $\dot{\nu} \sim 10^{-16}$ Hz s^{-1}. Efforts to constrain the X-ray frequency evolution to date have met with mixed success, principally due to the sparseness of earlier observations. Here we describe the results of the first phase coherent X-ray monitoring campaign on RX J0806.3+1527 with *Chandra*. We obtained a total of 70 ksec of exposure in 6 epochs logarithmically spaced over 320 days. With these data we conclusively show that the X-ray frequency is increasing at a rate of $3.77 \pm 0.8 \times 10^{-16}$ Hz s^{-1}. Using the ephemeris derived from the new data we are able to phase up all the earlier *Chandra* and ROSAT data and show they are consistent with a constant $\dot{\nu} = 3.63 \pm 0.06 \times 10^{-16}$ Hz s^{-1} over the past decade. This value appears consistent with that recently derived by Israel et al. largely from monitoring of the optical modulation, and is in rough agreement with the solutions reported initially by Hakala et al., based on ground-based optical observations. The large and stable $\dot{\nu}$ over a decade is consistent with gravitational radiation losses driving the evolution. An intermediate polar (IP) scenario where the observed X-ray period is the spin period of an accreting white dwarf appears less tenable because the observed $\dot{\nu}$ requires an $\dot{m} \approx 4 \times 10^{-8}$ $M_{\odot}$ yr^{-1}, that is much larger than that inferred from the observed X-ray luminosity (although this depends on the uncertain distance and bolometric corrections), and it is difficult to drive such a high $\dot{m}$ in a binary system with parameters consistent with all the multiwavelength data. If the ultracompact scenario is correct, then the X-ray flux cannot be powered by stable accretion which would drive the components apart, suggesting a new type of energy source (perhaps electromagnetic) may power the X-ray flux.

Subject headings: Binaries: close - Stars: individual (RX J0806.3+1527, V407 Vul) - Stars: white dwarfs – X-rays: binaries – Gravitational Waves

1. Introduction

The influence of gravitational radiation emission on binary evolution is most easily perceived in very close binaries. Double degenerate systems containing a pair of white dwarfs are the most compact systems known and can theoretically have orbital periods shorter than 5 minutes (Warner 1995; Tutukov & Yungelson 1996; Nelemans et al. 2001). Two candidate double degenerate systems have been the focus of much research over the last few years; V407 Vul (also known as RX J1914.4+2456), and RX J0806.3+1527 (hereafter J0806). Both objects were discovered in the ROSAT survey (Beuermann et al. 1999), and they share much in common (see Cropper et al. 2003 for a recent review). Each shows a periodic, $\approx$ 100% X-ray modulation with a sharp rise and more gradual decline. The observed X-ray periods are 9.5 and 5.4 minutes for V407 Vul and J0806, respectively. They are also optically variable at these same periods, and the optical lightcurves lag their X-ray profiles by about 1/2 a cycle, strongly suggesting that the optical variations result from X-ray heating of the secondary in a phase-locked, synchronized binary (Ramsay et al. 2000; Israel et al. 2003; Israel et al. 2004).

Although the current "even money" bet is that the observed periods in these systems represent the orbital periods of ultracompact systems, there is still no direct detection of orbital motion, as would be provided by observations of Doppler shifted spectral lines, for example. Scenarios associating the observed periods with the spin of a white dwarf are not completely ruled out, but are highly constrained. For example, recent optical and near-IR photometry of J0806 strongly constrains the nature of its secondary. Only an implausibly large distance would allow a low mass, main-sequence secondary (Reinsch, Burwitz & Schwarz 2004). This poses difficulties for an intermediate polar (IP) interpretation for J0806 (Norton, Haswell & Wynn 2004). Other challenges for such models are the extremely soft X-ray spectrum (Israel et al. 2003), and the lack of any detection of the longer orbital period that is usually seen in IPs.

Important constraints on models for these systems can be obtained by measuring their frequency evolution. If the systems are Roche lobe accretors, and the mass donors are degenerate, then stable accretion will lead to a widening of the orbit and a decrease in the orbital frequency, ie. $\dot{\nu} < 0$ (Strohmayer 2002; Marsh, Nelemans & Steeghs 2004). This is contrary to what has been observed to date. Based on a timing study of archival ROSAT and ASCA data Strohmayer (2002) found evidence that the orbital frequency of V407 Vul is increasing at a rate consistent with loss of orbital angular momentum to gravitational radiation. More recent monitoring of the system with *Chandra* and XMM-Newton confirms the initial evidence for spin-up (Strohmayer 2004; Ramsay et al. 2005). Hakala et al. (2003, 2004) have used archival ROSAT and optical timing measurements of J0806 to attempt to constrain its frequency evolution. Using noncoherent methods they found evidence for a frequency derivative, $\dot{\nu}$, of either about 3 or 6×10^{-16} Hz s^1, but could not unambiguously measure the rate due to the sparseness of available observations. Strohmayer (2003) explored whether the early ROSAT data and a single, more recent *Chandra* observation were consistent with the range of $\dot{\nu}$ values found by Hakala et al. (2003). He concluded they were, and found weak evidence favoring the higher $\dot{\nu}$ solution. More recently, Israel et al. (2004) have recently reported results from an optical monitoring campaign to explore the frequecy evolution of J0806. They obtained sufficient optical coverage to perform a coherent timing analysis and find a positive $\dot{\nu} = 3.5 \pm 0.1 \times 10^{-16}$ Hz s^{-1}. Using their coherent optical solution they were able to show that existing X-ray observations were also consistent with this solution.

The current timing results suggest that either accretion does not power the X-ray flux, or perhaps the donors are non-degenerate. This latter alternative also appears unlikely, especially for J0806, simply because so compact a system could not contain such a donor (Savonije, de Kool & van den Heuvel 1986). If the systems are detached and ultracompact then the question arises as to the source of the X-ray emission. An interesting possibility, suggested by Wu et al. (2002), is that these objects are "electric" stars, powered by unipolar induction. In such a scenario the primary is magnetized and a small asynchronism between the primary and secondary induces an electromotive force that drives currents between the components. This process can heat a small polar cap on the primary, thus producing X-ray emission. Although difficulties with the details of this model exist it has the attractive feature that the orbital spin-up is dominated by the loss of gravitational radiation. In light of the remaining uncertainties regarding the nature of these objects and the interesting implications of timing constraints, it is important to continue temporal monitoring of these objects in both the optical and X-ray domain.

Here we report results of the first phase coherent X-ray timing campaign for J0806 using *Chandra*. We obtained a total of 70 ksec of exposure in 6 logarithmically spaced epochs spanning 320 days. The observing plan was designed to maintain phase coherence assuming $\dot{\nu}$ was as large as $\approx 10^{-15}$ Hz s^{-1}. We show that the new *Chandra* data conclusively establish that the X-ray frequency of J0806 is increasing at a rate of $\approx 3.6 \times 10^{-16}$ at the present epoch. We use our new ephemeris to phase connect earlier *Chandra* and ROSAT data and show that the source has been spinning up at a more or less constant rate over the past decade. We discuss the implications of the now secure conclusion that the X-ray and optical frequencies are phase locked and are increasing at a large rate consistent with that expected due to gravitational radiation from a detached, ultracompact binary. We argue that spin-up of an accreting white dwarf appears increasingly unlikely because the large accretion rate required is inconsistent with the modest inferred X-ray luminosity and the difficulty of driving so high a mass transfer rate in a system consistent with all the multiwavelength constraints.

2. Data Extraction and Analysis

We observed J0806 with *Chandra* on six occasions from January 5, 2004 to November 22, 2004. We used ACIS-S in continuous clocking (CC) mode in order to mitigate pile-up. We used the backside-illuminated (S3) chip to maximize the soft photon response. Table 1 contains a summary of the observations. To prepare the data for our timing analysis, we first corrected the detector readout times to arrival times using the *Chandra* X-Ray Center's (CXC) analysis thread on timing with CC mode data. We then corrected the arrival times to the solar system barycenter using the CIAO tool *axbary* with the JPL-DE405 ephemeris. We used the source position, $\alpha = 08^h06^m23^s.2$, $\delta = 15°27'30''.2$, which is consistent with both optical and X-ray observations (Ramsay, Hakala & Cropper 2002; Israel et al. 2002; Israel et al. 2003). This process produced a set of photon arrival times in the barycentric dynamical time system (TDB).

The CC mode produces a one-dimensional "image" of the sky exposed to the detectors. An example image for the 2004, January 5 observation is shown in Figure 1. Photons from J0806 produce the strong peak in the plot. We carried out the same image analysis for all observations and extracted only events from within the source peaks for our timing study. Figure 2 shows a portion of a light curve produced from source extracted events and demonstrates that *Chandra* easily detects individual pulses from the source. We carried out this procedure on all the data and obtained a total of 15,418 photon events for our timing analysis.

2.1. Coherent Timing Solutions

We performed a coherent timing analysis using the Z_n^2 statistic (Buccheri 1983; see also Strohmayer 2004 and Strohmayer & Markwardt 2002 for examples of the use of this statistic in a similar context). To model the arrival times of pulses we use a two parameter phase model, $\phi(t) = \nu_0(t - t_0) + \frac{1}{2}\dot{\nu}(t - t_0)^2$. Here, ν_0 is the frequency at the reference epoch, t_0, and $\dot{\nu}$ is a constant frequency derivative. Since details of the method are described elsewhere we do not repeat them here.

We began by computing Z_3^2 as a function of ν_0 assuming a model with $\dot{\nu} \equiv 0$. This is more or less equivalent to a power spectrum analysis. The results are shown in Figure 3. The best constant frequency is 3.1101430 mHz, and there is no ambiguity with regard to identifying the correct frequency. That is, sidebands caused by the gaps in the data are at vastly less significant values of Z_3^2 (see Strohmayer 2004). We next computed a set of phase residuals using this constant frequency model (see Figure 5, upper panel). This $\dot{\nu} \equiv 0$ model does not fit the phases well, indeed, the need for a positive $\dot{\nu}$ is indicated in this plot by the downward opening quadratic trend in the residuals.

We next included non-zero $\dot{\nu}$ values in the model and performed a grid search by calculating χ^2 at each ν_0 - $\dot{\nu}$ pair (see Strohmayer 2004 for details of the method). The results are summarized in Figures 4 and 5. Figure 4 shows the 68% and 90% confidence contours (dashed) in the ν_0 - $\dot{\nu}$ plane. We find a best fitting solution of $\nu_0 = 3.1101380 \pm 0.0000006$ mHz and $\dot{\nu} = 3.77 \pm 0.8 \times 10^{-16}$ Hz s^{-1}, using a reference epoch of $t_0 = 53009.889943753$ MJD (TDB). Errors here are 1σ. The fit is excellent, with a minimum $\chi^2 = 48.9$ with 51 degrees of freedom (dof). Fixing $\dot{\nu}$ at zero results in an increase in χ^2 of about 87, which strongly excludes the constant frequency model. These calculations demonstrate conclusively that J0806 is indeed spinning up. Figure 5 shows two set of phase residuals. As noted above, the top panel shows the residuals obtained from the best constant frequency ($\dot{\nu} = 0$) model, and the bottom panel shows the best solution with a positive $\dot{\nu}$.

With an accurate solution in hand we can project backwards in time to the epoch of the earliest *Chandra* and ROSAT observations of J0806 (these data were discussed previously by Strohmayer 2003; Israel et al. 2003; and Hakala et al. 2003). We first included the November, 2001 *Chandra* data, and recomputed χ^2 on our ν_0 - $\dot{\nu}$ grid. The results are also shown in Figure 4 (solid contours, again, 68% and 90% confidence). As can be seen, the November, 2001 *Chandra* data are entirely consistent with the solution derived from our 2004 data (dashed contours), but the longer baseline provides much tighter constraints on the parameters. Combining all the *Chandra* data we find $\nu_0 = 3.11013824 \pm 0.00000017$ mHz and $\dot{\nu} = 3.63 \pm 0.06 \times 10^{-16}$ Hz s^{-1}, using the same reference epoch. This solution is very close to that reported by Israel et al. (2004) based primarily on their optical monitoring campaign.

We show two representations of the phase residuals using all the *Chandra* data. Figure 6 shows the phase residuals with respect to a constant frequency ($\dot{\nu} = 0$) model, and further demonstrates that a quadratic trend (positive $\dot{\nu}$) is clearly needed to model all the phases. Figure 7 shows the phase residuals using our best ν_0 - $\dot{\nu}$ model. This model accurately describes all the *Chandra* phase timings, and has an rms residual of less than 0.01 of a cycle (horizontal dashed lines). We note that this solution is also consistent with the earliest ROSAT data, but the inclusion of those data do not appreciably tighten the constraints because the contributions to χ^2 are dominated by the more numerous and higher signal to noise ratio *Chandra* measurements. Finally, we phase folded all the *Chandra* data using our best timing solution, and the resulting modulation profile is shown in Figure 8.

3. Discussion and Implications

Based on the Israel et al. (2004) study and the present work, it is now undeniable that the X-ray and optical modulations of J0806 are stable, phase-locked and speeding up at a rate consistent with what would be expected for gravitational radiation losses in an ultracompact binary. What still has not been demonstrated conclusively is that the observed period is indeed orbital in nature. If the period is not orbital, the only remaining plausible model would seem to be accretion-induced spin-up of a white dwarf, most likely in a nearly face-on IP system similar to that described by Norton, Haswell & Wynn (2004). Assuming this model is correct one can estimate the accretion rate required to account for the observed spin-up. To order of magnitude the accretion-induced spin-up rate is,

$$I\dot{\omega} = \dot{m}\,(GMr_c)^{1/2} \ . \qquad (1)$$

Here, I, $\dot{\omega} = 2\pi\dot{\nu}$, $\dot{m}$, M, and r_c are the stellar moment of inertia, the spin angular frequency derivative. the mass accretion rate, the stellar mass, and the characteristic radius at which the accreted matter is "captured" by the star (effectively the lever arm over which the torque acts). Assuming $I = \frac{2}{5}MR^2$, with R the stellar radius, we can express the mass accretion rate as,

$$\dot{m} = \frac{4\pi}{5}\dot{\nu}\left(\frac{MR^4}{Gr_c}\right)^{1/2} \ . \qquad (2)$$

Plugging in our measured $\dot{\nu}$, assuming $M = 0.5M_{\odot}$, using the Zapolsky & Salpeter (1969) mass-radius relation, and taking $r_c = R$ we obtain a characteristic value of $\dot{m} \approx 4 \times 10^{-8}$ $M_{\odot}$ yr^{-1}. This would provide an accretion luminosity, $L_{acc} = GM\dot{m}/R$ of about 2×10^{35} ergs s^{-1}, which is equivalent to a flux (at 500 pc) of $f_{acc} \approx 6 \times 10^{-9}$ ergs cm^{-2} s^{-1}.

We are still in the process of carrying out a spectral study of our CC-mode data (ACIS CC-mode is still only crudely calibrated for spectroscopy), however, Israel et al. (2003) have done a spectral analysis of the ACIS-S imaging data from November, 2001. Assuming the source spectrum has not changed dramatically over time we can use their spectral parameters to scale our observed count rates to X-ray fluxes. They found a peak, unabsorbed X-ray flux in the 0.1 - 2.5 keV band of 1.5×10^{-11} ergs cm^{-2} s^{-1}. We calculated average count rates for each of our observations and show them plotted versus time in Figure 9. Our brightest epoch had an average rate of 0.26 s^{-1}, and the time history shows $\approx$ 50% variations in intensity. For comparison, the average count rate during the November, 2001 observations reported by Israel et al. (2003) was 0.29 s^{-1}, a bit higher than in our more recent observations. We note that recent count rates could be reduced somewhat by the additional build-up of a contaminant on the ACIS detectors (Marshall et al. 2004). We also note that spectral results obtained recently using XMM-Newton data give comparable flux levels (Israel et al. 2004).

The observed X-ray fluxes from J0806 are, at a minimum, several orders of magnitude less than the total accretion luminosity expected if we are seeing accretion-induced spin-up of a white dwarf. We note that larger, previously measured fluxes do not falsify this argument because we have measured the spin-up rate and fluxes over the same epoch. Although it is possible that a significant fraction of the accretion luminosity appears outside the X-ray band–particularly in the extreme UV–it seems unlikely that this can explain all of the mismatch. As noted by Israel et al. (2003), sensitive EUV observations of the source would be very revealing on this score. A second caveat is the uncertain distance. The most recent spectral study with XMM-Newton suggests the absorption column is consistent with the Galactic value in the direction to J0806 (Israel et al. 2004). This implies that unless the source is very far out of the galactic plane its distance is probably not much greater than about 500 pc. The fact that its proper motion is small provides some evidence that it is not a halo object and therefore is not too far out of the Galactic plane (Israel et al. 2002).

Another question which might be asked is whether an IP system with an orbital period somewhat longer than one hour (as suggested by Norton et al. 2004), and with a very late type secondary consistent with the optical and infrared photometry can in fact transfer mass at the rate required to match the observed spin up? It appears likely that in such a system angular momentum losses due to gravitational radiation would be insufficient to account for such a large mass transfer rate. This is because gravitational radiation driven mass loss is a very sensitive function of orbital frequency and secondary mass (Rappaport et al. 1982; Priedhorsky & Verbunt 1988; Marsh, Nelemans & Steeghs 2004). With an orbital period longer than 1 hr, and a secondary later than M6 (Reinsch et al. 2004), a system with stellar parameters appropriate for an IP interpretation of J0806 would have a long term mass transfer rate driven by gravitational radiation of $\dot{m}_{gr} \approx 5 \times 10^{-11}$ $M_{\odot}$ yr^{-1}, which is much smaller than required to achieve the observed spin up rate in J0806. Indeed, a class of binaries with these characteristic transfer rates are the recently discovered accreting millisecond pulsars, with orbital periods from 40 min to a few hours, and very low mass secondaries (see Wijnands 2004 for a recent review). The main difference between these systems and a putative IP scenario for J0806 would seem to be that their primaries are neutron stars and not white dwarfs. Perhaps other mechanisms can drive mass transfer at the required rate, such as magnetic braking, but there appears to be a lot of ground to make up.

If the observed period is orbital then the system is a powerful source of gravitational radiation. Indeed, a circular binary with component masses m_1 and m_2 separated by a distance a will radiate a gravitational wave luminosity (Peters & Matthews 1963),

$$L_{gw} = \frac{32G^4}{5c^5}\frac{m_1^2 m_2^2(m_1+m_2)}{a^5} \ . \tag{3}$$

Taking $m_1 = m_2 = 0.5M_\odot$ and a separation consistent with the observed period one finds $L_{gw} \approx 1 \times 10^{35}$ ergs s^{-1}, which is substantially larger than the observed X-ray flux.

4. Summary and Conclusions

Our *Chandra* monitoring of J0806 confirms that its X-ray frequency is increasing at a rate of 3.6×10^{-16} Hz s^{-1}. Our results are in agreement with the independent optical monitoring campaign carried out by Israel et al. (2004). These studies show that the X-ray and optical modulations are phase-locked and stable over more than a decade. Although direct confirmation that the observed period is orbital in nature is still lacking, we believe that the present evidence strongly favors an orbital interpretation. If this is the case, then we are seeing the influence of gravitational radiation losses on the most compact binary known. Indeed, the rate of change of its orbital frequency would be $\approx 10^5$ times larger than that of the famous binary pulsar (Taylor & Weisberg 1989).

Because of the remaining uncertainties and the importance of this object in the context of directly observing gravitational radiation driven orbital evolution, and perhaps studying a new form of stellar energy (ie. electric stars), additional observations are extremely important. Deep phase resolved optical and X-ray spectroscopy might reveal radial velocity variations consistent with orbital motion. Sensitive EUV data would be helpful in constraining the overall energy budget and thus bounding the accretion rate. Continued X-ray and optical timing are essential to further study the torque and phase stability. Finally, if further electromagnetic observations do not prove definitive, then observations with a future space-based gravitational radiation detector, such as the NASA/ESA LISA mission currently in development, would provide a final test of the ultracompact hypothesis. Indeed, if the observed period is orbital, then the source will produce a strong gravitational radiation signal at twice the observed electromagnetic frequency, and LISA should be able to detect it easily. LISA observations could also provide the distance and inclination of the system. With such information in hand, an intimate portrait of the evolution and energetics of the system would emerge.

References

Beuermann, K. et al. 1999, A&A, 347, 47.

Buccheri, R. et al. 1983, A&A, 128, 245.

Cropper, M., Ramsay, G., Wu, K. & Hakala, P. 2003, in Proc. Third Workshop on Magnetic CVs, Cape Town, (astro-ph/0302240).

Hakala, P., Ramsay, G. & Byckling, K. 2004, MNRAS, 353, 453.

Hakala, P. et al. 2003, MNRAS, 340, L10.

Israel, G. L. et al. 2004, Proceedings of the XLVII National Conference of the S.A.It., Mem.S.A.It. Suppl., Eds. A. Wolter, G.L. Israel & F. Bacciotti, (astro-ph/0410453).

Israel, G. L. et al. 2003, apJ, 598, 492.

Israel, G. L. et al. 2002, A&A, 386, L131.

Israel, G. L. et al. 1999, A&A, 349, L1.

Marsh, T. R., Nelemans, G. & Steeghs, D. 2004, MNRAS, 350, 113.

Marshall, H. L., Tennant, A., Grant, C. E., Hitchcock, A. P., O'Dell, S. L., & Plucinsky, P. P. 2004, Proc. SPIE, 5165, 497.

Nelemans, G., Portegies Zwart, S. F., Verbunt, F. & Yungelson, L. R. 2001, A&A, 368, 939.

Norton, A. J., Haswell, C. A. & Wynn, G. A. 2004, A&A, 419, 1025.

Peters, P. C., & Mathews, J. 1963, Physical Review , 131, 435.

Priedhorsky, W. C. & Verbunt, F. 1988, ApJ, 333, 895.

Ramsay, G., Cropper, M., Wu, K., Mason, K. O., & Hakala, P. 2000, MNRAS, 311, 75.

Ramsay, G., Hakala, P. & Cropper, M. 2002, MNRAS, 332, L7.

Ramsay, G., et al. 2002, MNRAS, 333, 575.

Rappaport, S., Joss, P. C. & Webbink, R. F. 1982, ApJ, 254, 616.

Reinsch, K., Burwitz, V. & Schwarz, R. 2004, To appear in RevMexAA(SC) Conference Series, Proc. of IAU Colloquium 194 'Compact Binaries in the Galaxy and Beyond', La Paz (Mexico), eds. G. Tovmassian & E. Sion, (astro-ph/0402458).

Savonije, G. J., de Kool, M., & van den Heuvel, E. P. J. 1986, A&A, 155, 51.

Strohmayer, T. E. 2004, ApJ, 610, 416.

Strohmayer, T. E. 2003, ApJ, 593, L39.

Strohmayer, T. E. 2002, ApJ, 581, 577.

Strohmayer, T. E., & Markwardt, C. B., 2002, ApJ, 577, 337.

Taylor, J. H. & Weisberg, J. M. 1989, ApJ, 345, 434.

Tutukov, A. & Yungelson, L. 1996, MNRAS, 280, 1035.

Warner, B. W. 1995, Cataclysmic Variable Stars (Cambridge: Cambridge Univ. Press).

Wijnands, R. 2004, in "X-ray Timing 2003: Rossi and Beyond," AIP Conference Proceedings vol. 714, ed. P. Kaaret, F. K. Lamb, & J. H. Swank, pg. 209.

Wu, K., Cropper, M., Ramsay, G. & Sekiguchi, K. 2002, MNRAS, 331, 221.

Zapolsky, H. S. & Salpeter, E. E. 1969, ApJ, 158, 809.

Figure Captions

Fig. 1.— *Chandra* one-dimensional image of J0806 from our January 5, 2004 (UTC) ACIS-S CC-mode observation. The sharp peak contains photons from the source.

Fig. 2.— Light curve of a portion of the *Chandra* ACIS-S data from the January 5, 2004 (UTC) observation of J0806. The bin size is 16 s, and ten individual pulses are shown.

Fig. 3.— Best constant frequency measurement for J0806 using all of our epoch 2004 *Chandra* observations. The Z_3^2 power spectrum is shown as a function of frequency in the vicinity of $\nu_0 = 3.11014250$ mHz.

Fig. 4.— Constraints on ν_0 and $\dot{\nu}$ for J0806 from our phase-timing analysis using the new, epoch 2004 *Chandra* dataset (dashed contours), and after combining the 2001 and 2004 datasets (solid contours). We show the joint 68% and 90% confidence regions in each case. The results definitively show that J0806 is spinning up at at rate of 3.6×10^{-16} Hz s^{-1}. Here $\nu_0 = 3.1101380$ mHz, and the reference epoch, $t_0 = 53009.889943753$ MJD (TDB).

Fig. 5.— Phase-timing residuals from our epoch 2004 monitoring observations of J0806. Plotted as a function of time are the residuals using the best constant frequency phase model (i.e., $\dot{\nu} = 0$; top panel), and with the best solution including a positive $\dot{\nu} = 3.77 \times 10^{-16}$ Hz s^{-1} (bottom panel). In the top panel a quadratic trend with the parabola opening downward is indicative of the need for a positive $\dot{\nu}$. The zero point on the time axis corresponds to $t_0 = 53009.889943753$ MJD (TDB).

Fig. 6.— Phase timing measurements for J0806 including the November, 2001 (UTC) *Chandra* observations. This plot shows how the phases drift with respect to a constant frequency model. The solid curve shows the spin-up model deduced from the 2004 epoch data, and is consistent with the phase timing of the epoch 2001 data.

Fig. 7.— Same as Figure 6 but now the model includes the best fit value of $\dot{\nu} = 3.63 \pm 0.06 \times 10^{-16}$ Hz s^{-1}. The horizontal dashed lines show the rms level of the residuals, which is less than 1/100 of a cycle.

Fig. 8.— Folded pulse profile for J0806 using the 2001 and 2004 *Chandra* data and our best timing solution. Phase zero is arbitray, and two cycles are shown for clarity. The horizontal dashed line is an estimate of the background in the 1-d images associated with the CC-mode data.

Fig. 9.— Average ACIS-S Count rates versus time from J0806 for our 2004 observations. Time is measured from $t_0 = 53009.889943753$ MJD (TDB). The mean rate is 0.219 s^{-1}, and

30% variations about this value are evident.

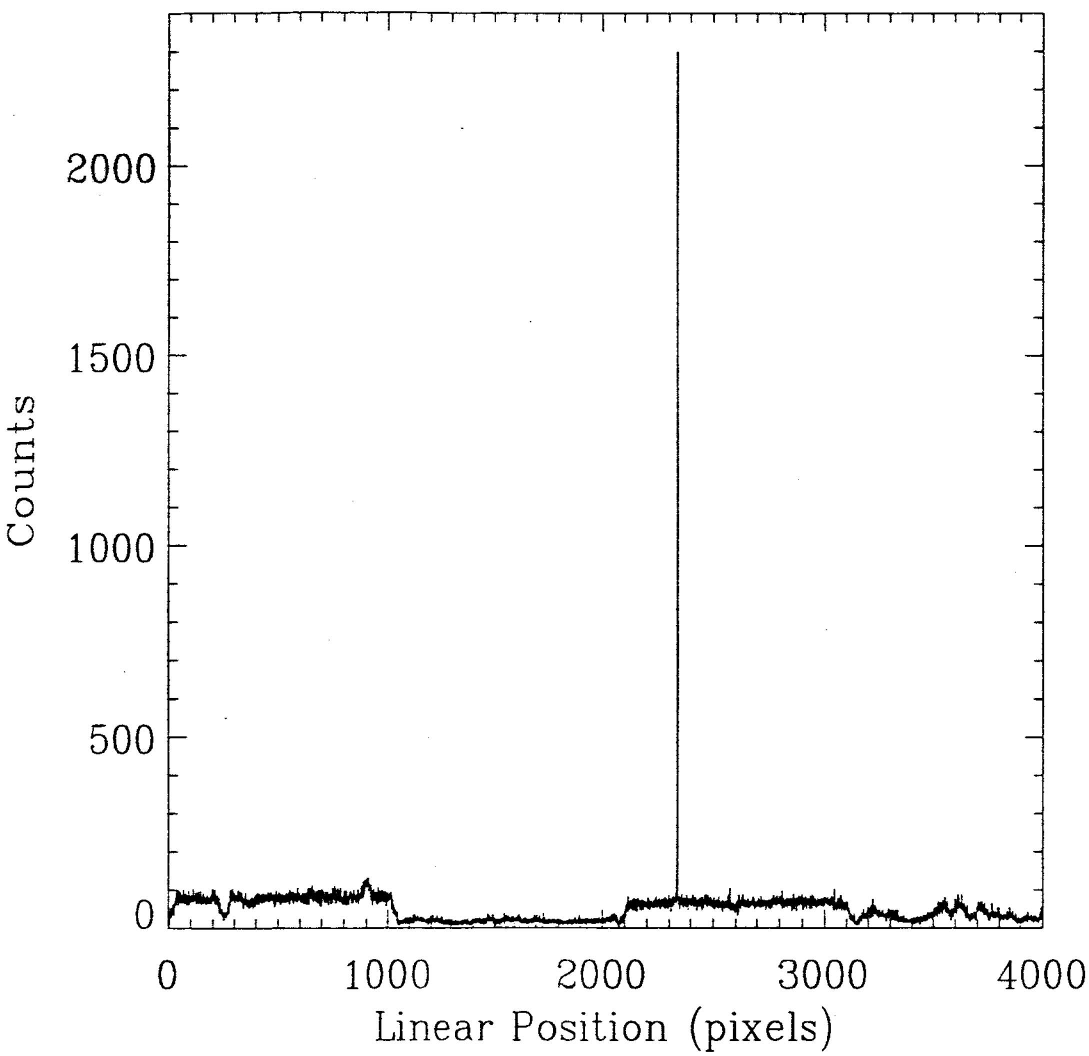

Figure 1: *Chandra* one-dimensional image of J0806 from our January 5, 2004 (UTC) ACIS-S CC-mode observation. The sharp peak contains photons from the source.

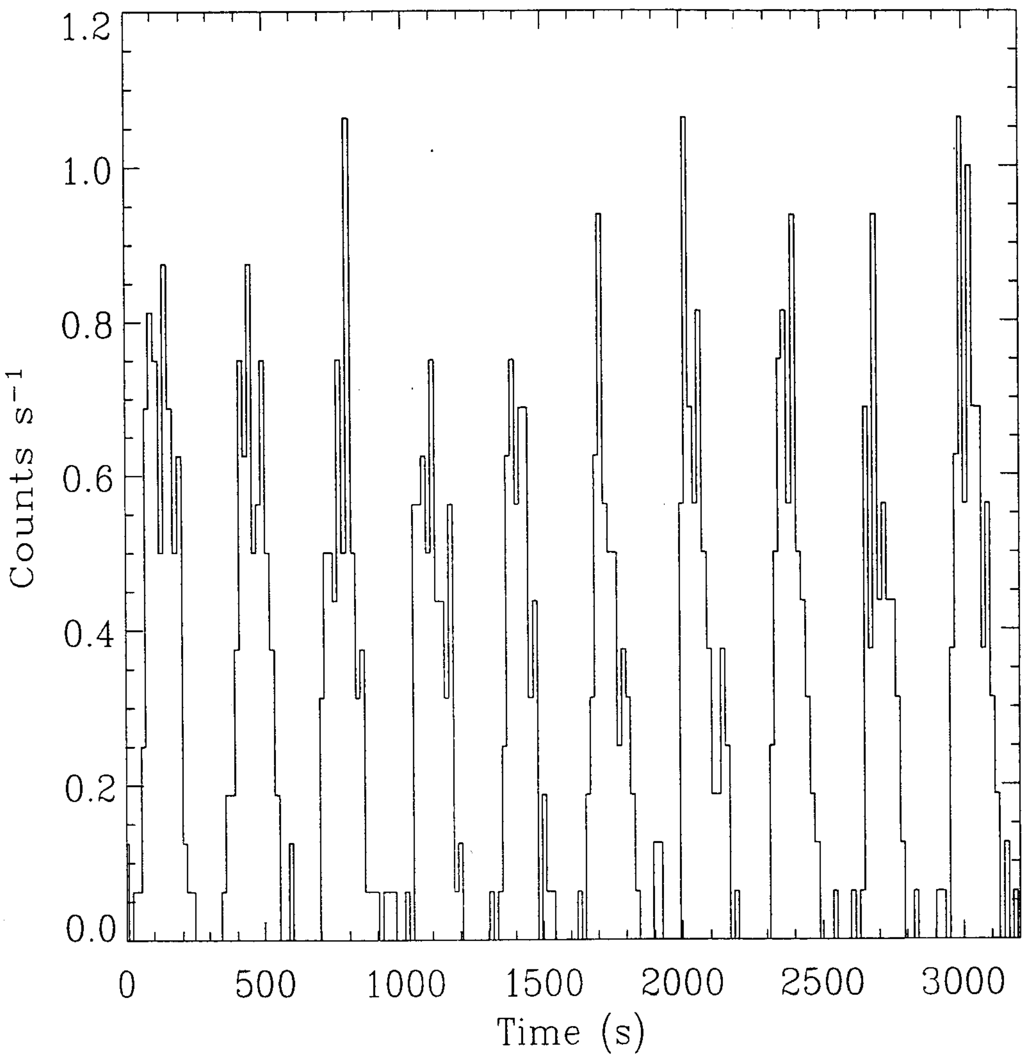

Figure 2: Light curve of a portion of the *Chandra* ACIS-S data from the January 5, 2004 (UTC) observation of J0806. The bin size is 16 s, and ten individual pulses are shown.

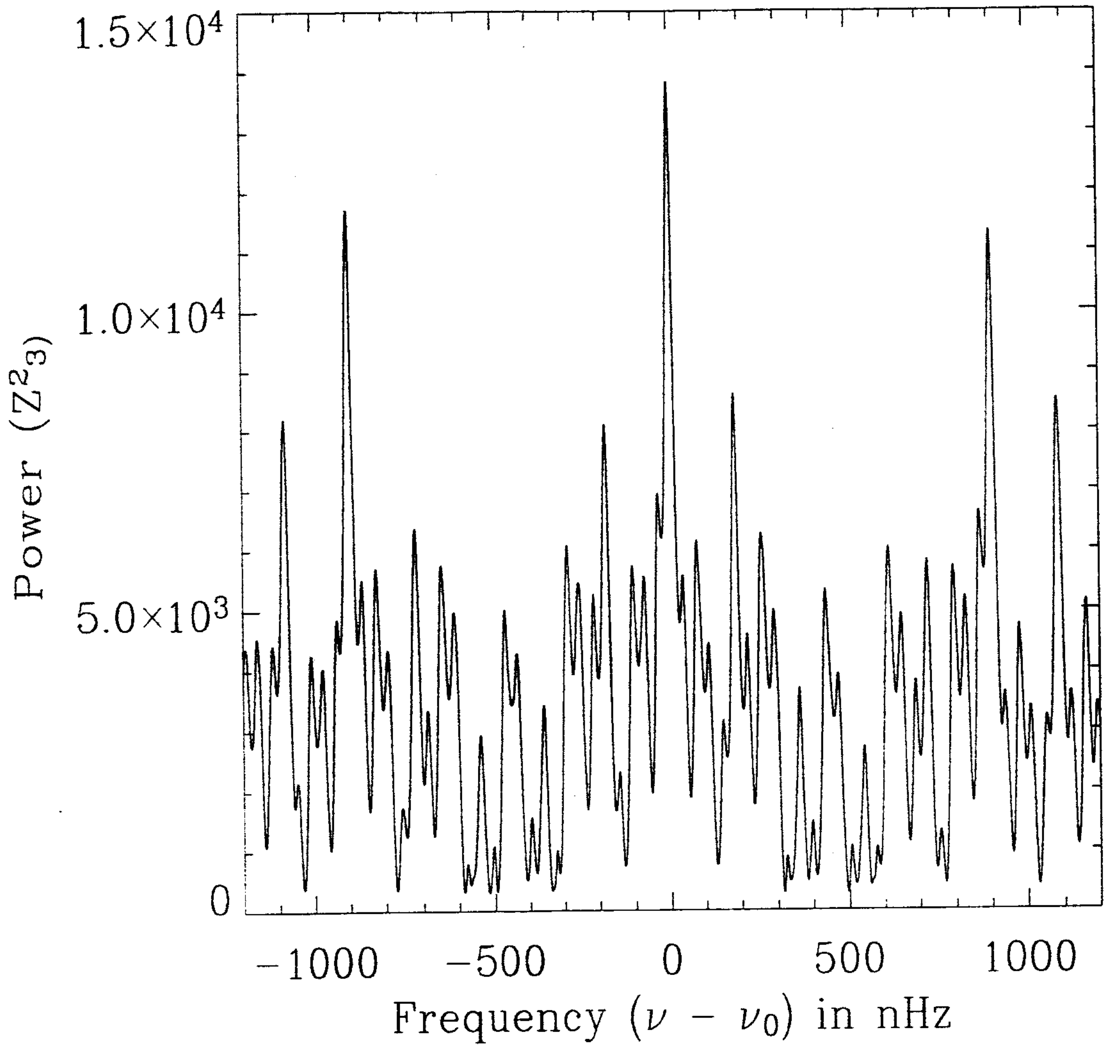

Figure 3: Best constant frequency measurement for J0806 using all of our epoch 2004 *Chandra* observations. The Z_3^2 power spectrum is shown as a function of frequency in the vicinity of $\nu_0 = 3.11014250$ mHz.

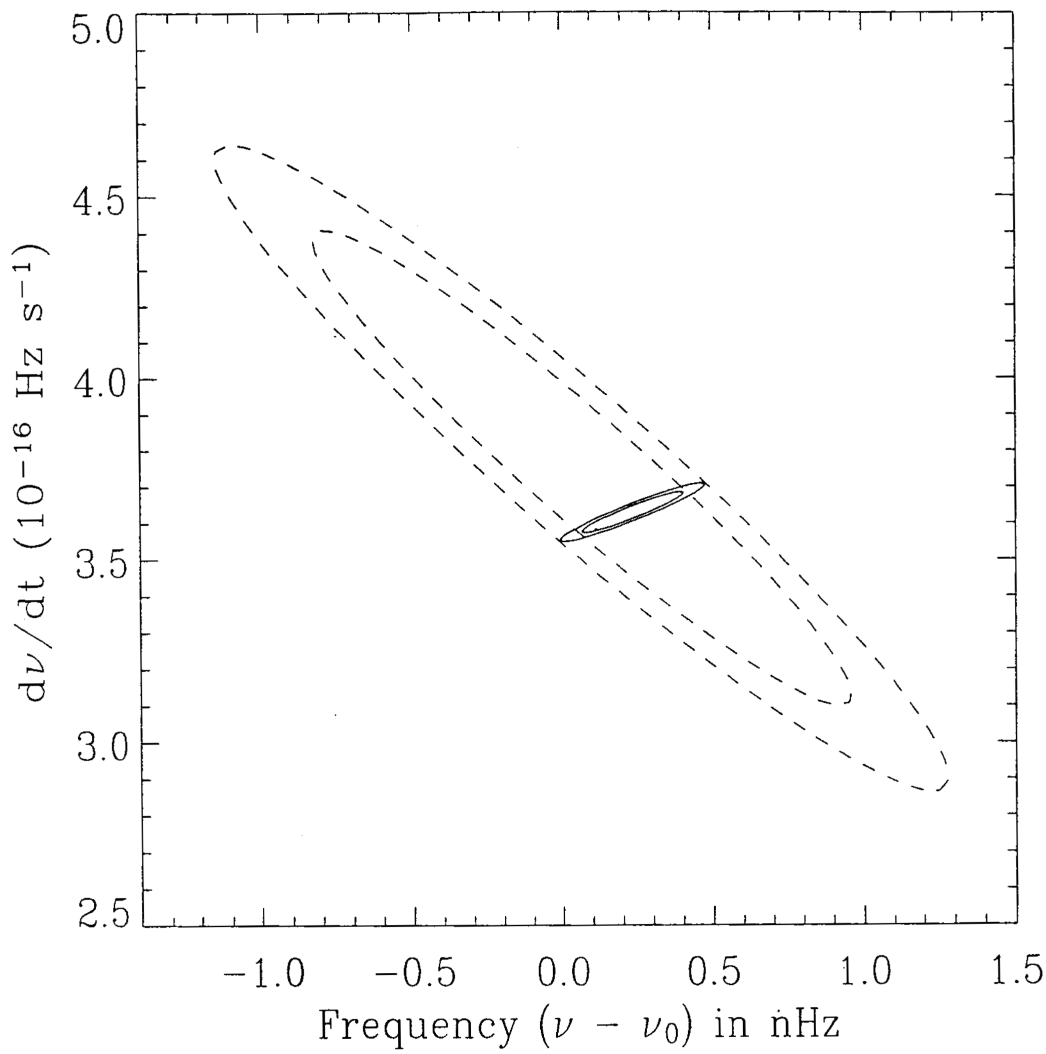

Figure 4: Constraints on ν_0 and $\dot{\nu}$ for J0806 from our phase-timing analysis using the new, epoch 2004 *Chandra* dataset (dashed contours), and after combining the 2001 and 2004 datasets (solid contours). We show the joint 68% and 90% confidence regions in each case. The results definitively show that J0806 is spinning up at at rate of 3.6×10^{-16} Hz s^{-1}. Here $\nu_0 = 3.1101380$ mHz, and the reference epoch, $t_0 = 53009.889943753$ MJD (TDB).

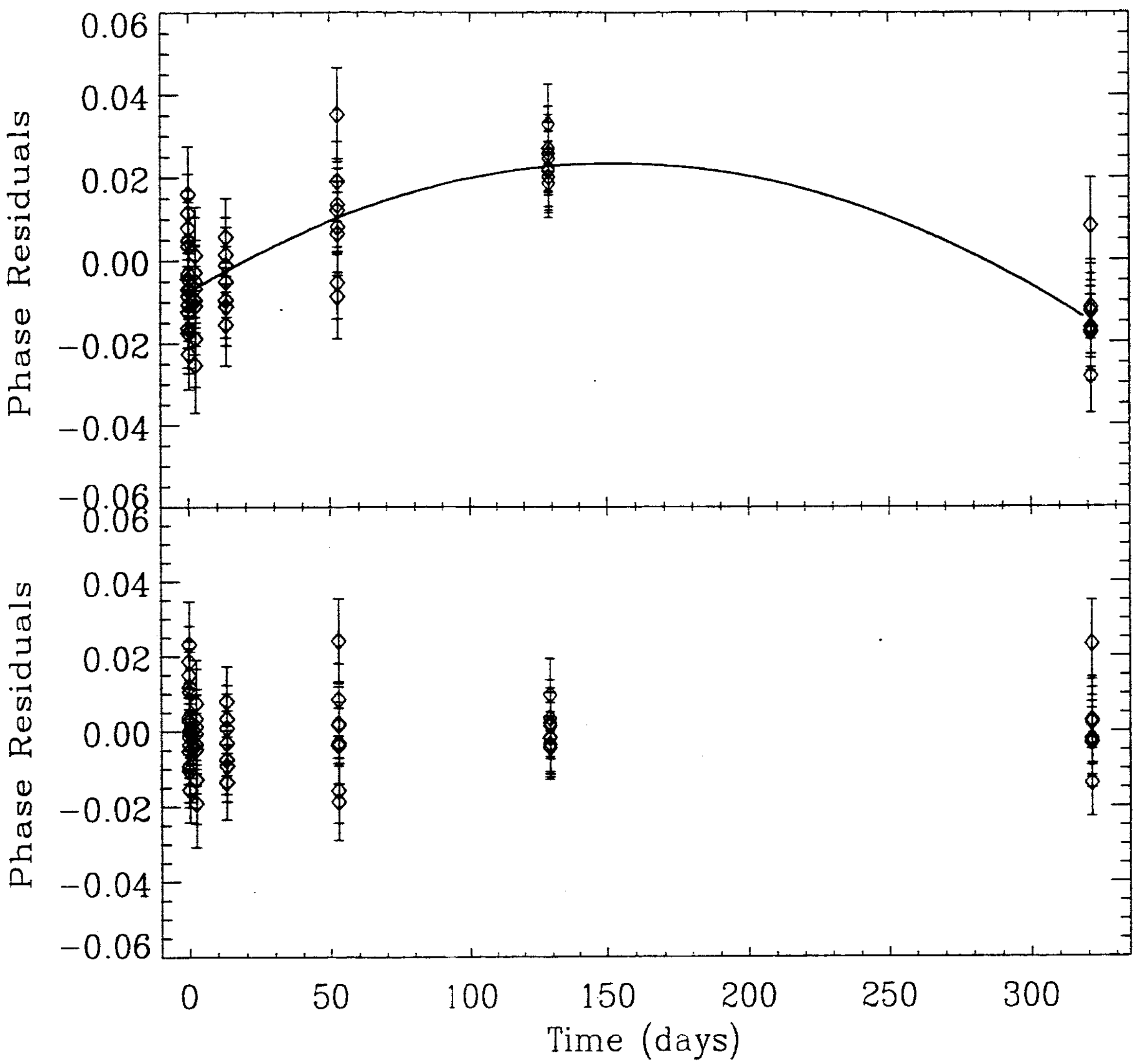

Figure 5: Phase-timing residuals from our epoch 2004 monitoring observations of J0806. Plotted as a function of time are the residuals using the best constant frequency phase model (i.e., $\dot{\nu} = 0$; top panel), and with the best solution including a positive $\dot{\nu} = 3.77 \times 10^{-16}$ Hz s^{-1} (bottom panel). In the top panel a quadratic trend with the parabola opening downward is indicative of the need for a positive $\dot{\nu}$. The zero point on the time axis corresponds to $t_0 = 53009.889943753$ MJD (TDB).

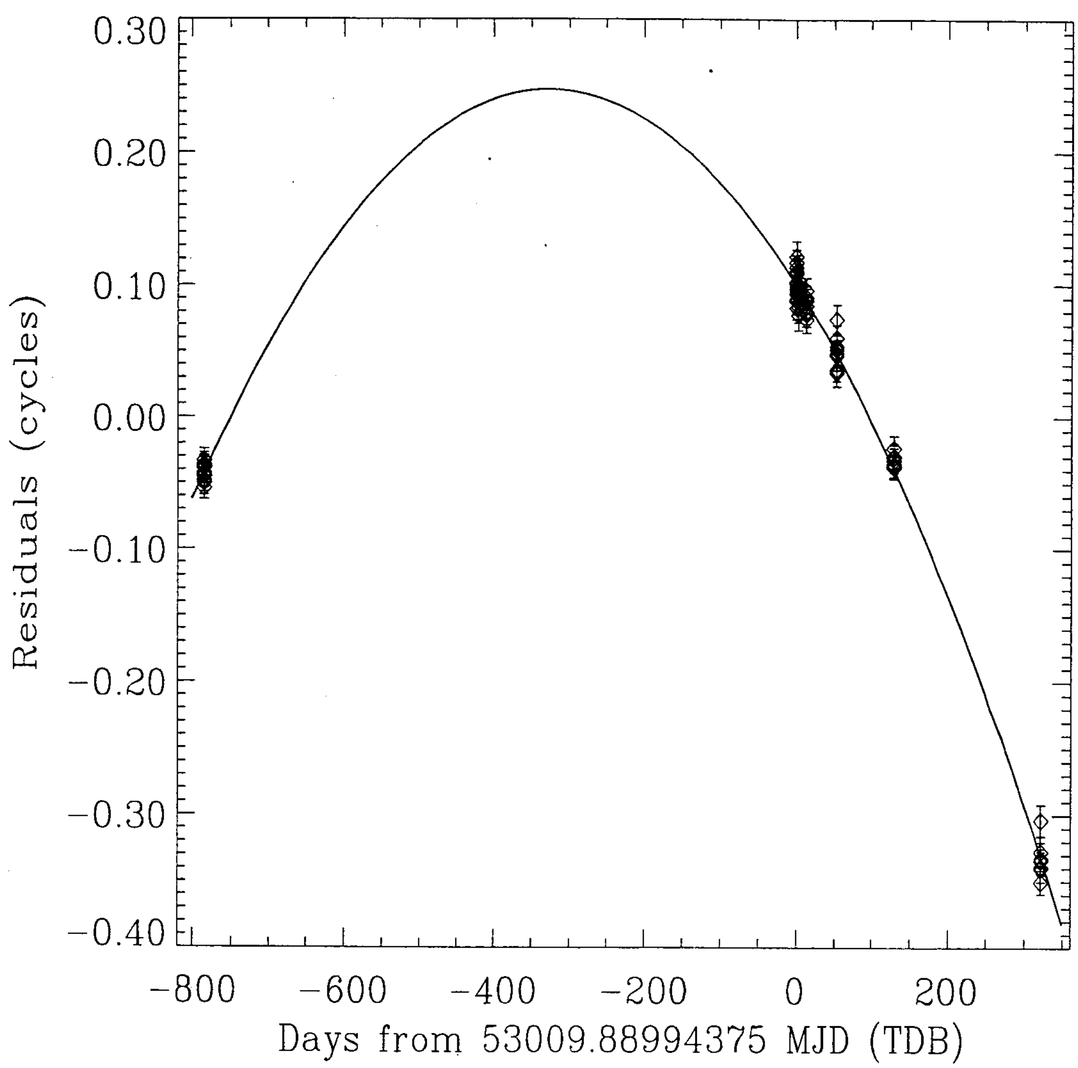

Figure 6: Phase timing measurements for J0806 including the November, 2001 (UTC) *Chandra* observations. This plot shows how the phases drift with respect to a constant frequency model. The solid curve shows the spin-up model deduced from the 2004 epoch data, and is consistent with the phase timing of the epoch 2001 data.

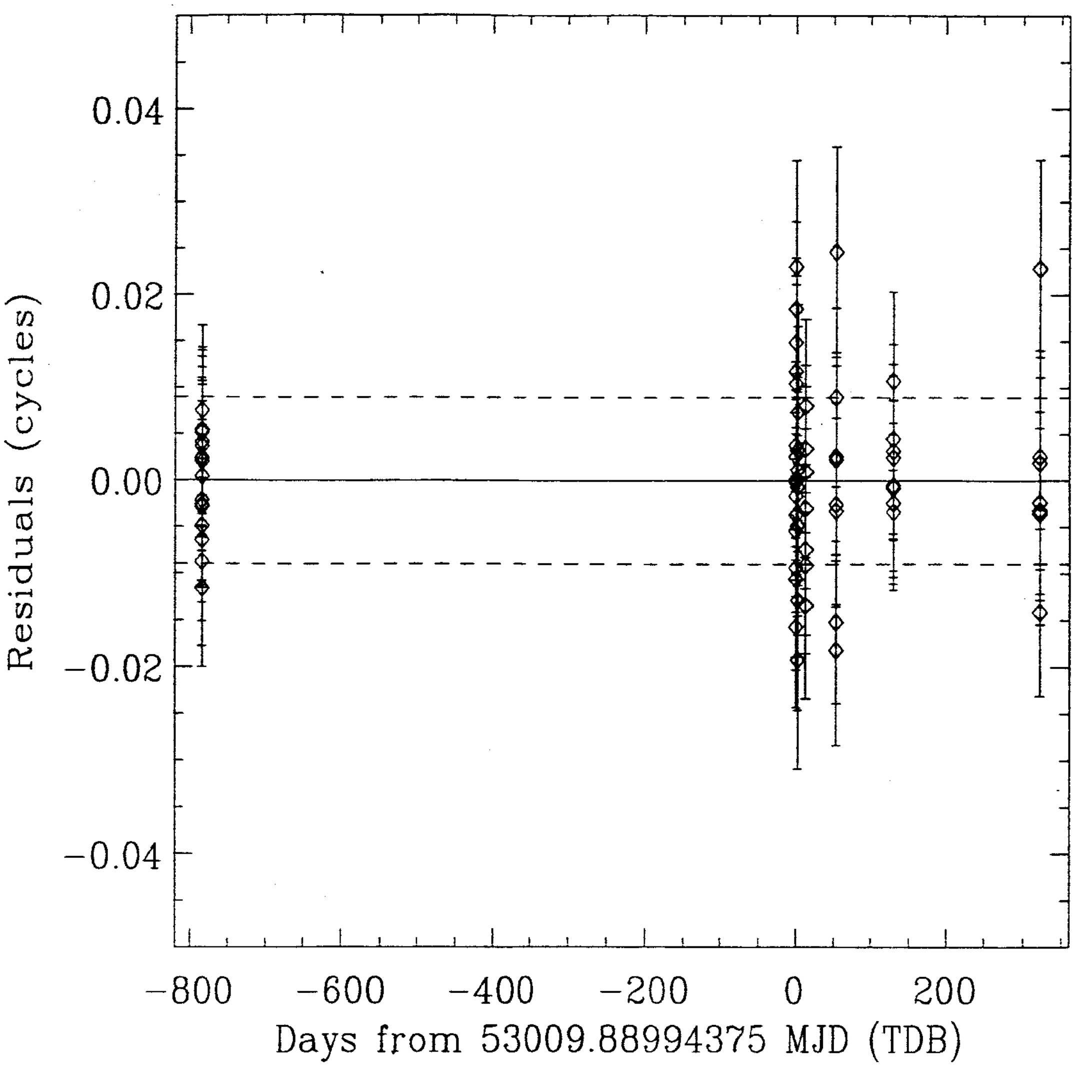

Figure 7: Same as Figure 6 but now the model includes the best fit value of $\dot{\nu} = 3.63 \pm 0.06 \times 10^{-16}$ Hz s^{-1}. The horizontal dashed lines show the rms level of the residuals, which is less than 1/100 of a cycle.

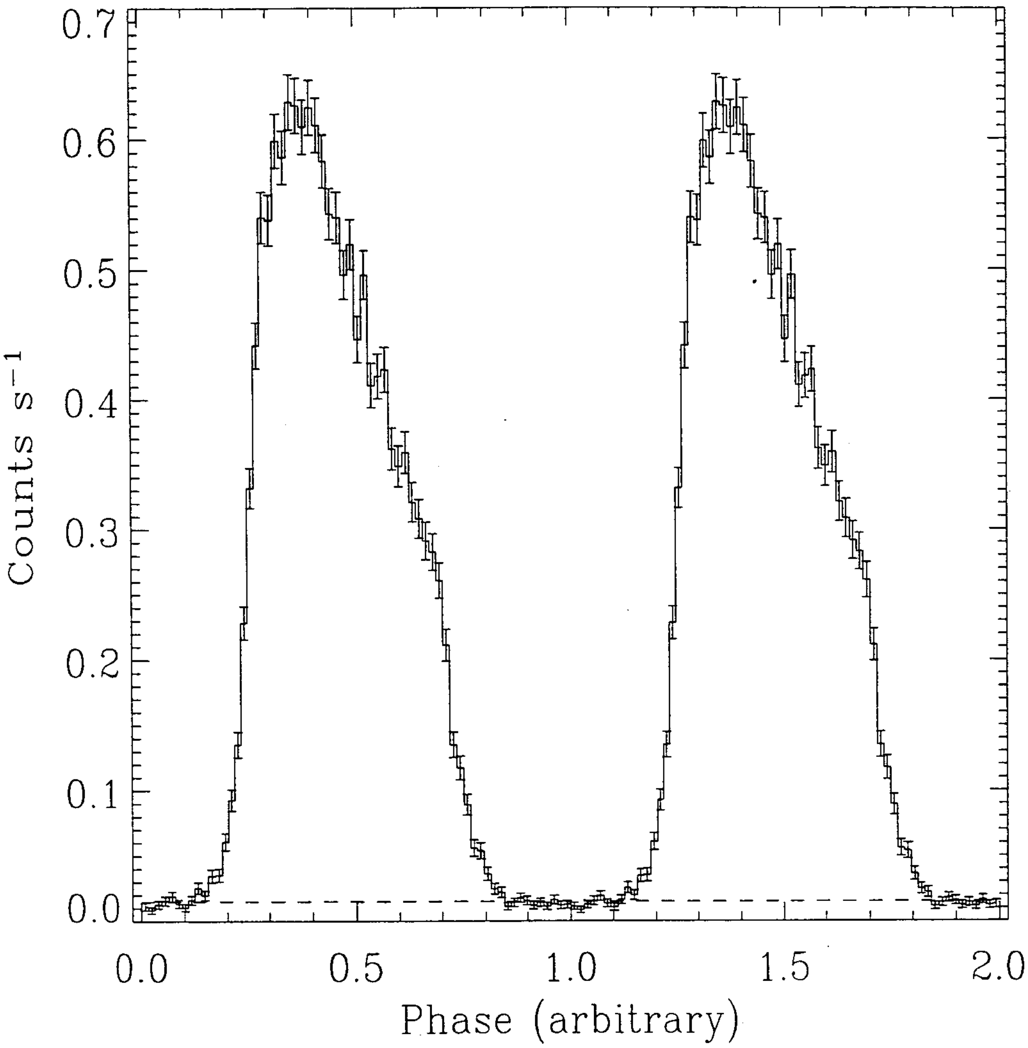

Figure 8: Folded pulse profile for J0806 using the 2001 and 2004 *Chandra* data and our best timing solution. Phase zero is arbitray, and two cycles are shown for clarity. The horizontal dashed line is an estimate of the background in the 1-d images associated with the CC-mode data.

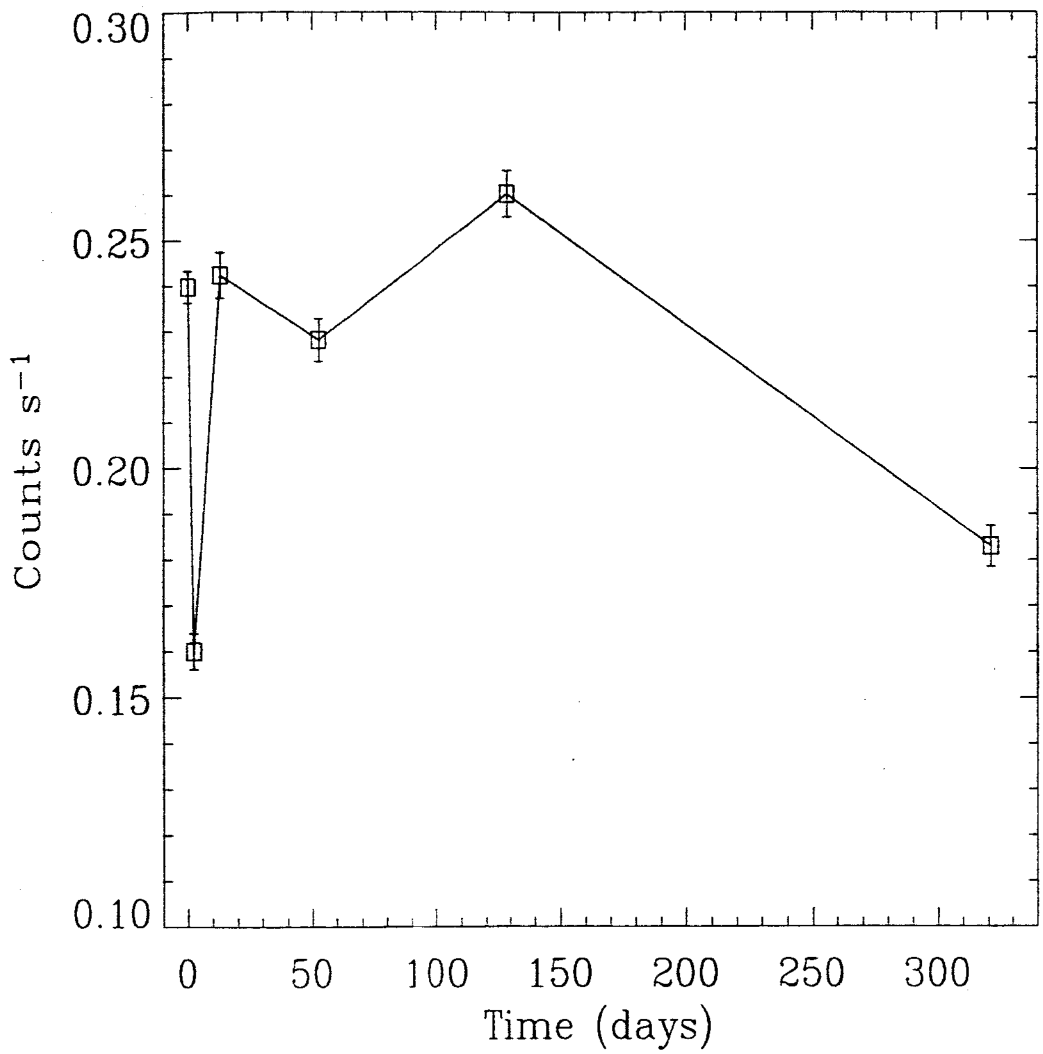

Figure 9: Average ACIS-S Count rates versus time from J0806 for our 2004 observations. Time is measured from $t_0 = 53009.889943753$ MJD (TDB). The mean rate is 0.219 s^{-1}, and 30% variations are evident.

Table 1: *Chandra* Observations of RX J0806.3+1527

	OBSID	Instrument	Start (TT)	Stop (TT)	Exp (ksec)
1	300117	ACIS-S (CC-mode)	Jan 05, 2004:21:02:50	Jan 06, 2004:02:47:15	19.5
2	300118	ACIS-S (CC-mode)	Jan 08, 2004:05:59:15	Jan 08, 2004:09:30:19	10.5
3	300119	ACIS-S (CC-mode)	Jan 18, 2004:22:55:48	Jan 19, 2004:02:02:29	9.8
4	300120	ACIS-S (CC-mode)	Feb 27, 2004:15:04:59	Feb 27, 2004:18:26:26	10.4
5	300121	ACIS-S (CC-mode)	May 13, 2004:21:25:04	May 14, 2004:00:44:47	10.2
6	300143	ACIS-S (CC-mode)	Nov 22, 2004:01:36:42	Nov 22, 2004:04:32:39	9.2